

# Non-Gaussianity from Axionic Curvaton

Masahiro Kawasaki,<sup>a,b1</sup> Takeshi Kobayashi,<sup>c,d2</sup> and Fuminobu Takahashi<sup>b,e3</sup>

<sup>a</sup> *Institute for Cosmic Ray Research, The University of Tokyo,  
5-1-5 Kashiwanoha, Kashiwa, Chiba 277-8582, Japan*

<sup>b</sup> *Institute for the Physics and Mathematics of the Universe, The University of Tokyo,  
5-1-5 Kashiwanoha, Kashiwa, Chiba 277-8582, Japan*

<sup>c</sup> *Canadian Institute for Theoretical Astrophysics, University of Toronto,  
60 St. George Street, Toronto, Ontario M5S 3H8, Canada*

<sup>d</sup> *Perimeter Institute for Theoretical Physics,  
31 Caroline Street North, Waterloo, Ontario N2L 2Y5, Canada*

<sup>e</sup> *Department of Physics, Tohoku University, Sendai 980-8578, Japan*

We study non-Gaussianity of density perturbations generated by an axionic curvaton, focusing on the case that the curvaton sits near the hilltop of the potential during inflation. Such hilltop curvatons can generate a red-tilted density perturbation spectrum without invoking large-field inflation. We show that, even when the curvaton dominates the Universe, the non-Gaussianity parameter  $f_{\text{NL}}$  is positive and mildly increases towards the hilltop of the curvaton potential, and that  $f_{\text{NL}} = \mathcal{O}(10)$  is a general and robust prediction of such hilltop axionic curvatons. In particular, we find that the non-Gaussianity parameter is bounded as  $f_{\text{NL}} \lesssim 30$ -40 for a range of the scalar spectral index,  $n_s = 0.94$ -0.99, and that  $f_{\text{NL}} = 20$ -40 is realized for the curvaton mass  $m_\sigma = 10$ - $10^6$  GeV and the decay constant  $f = 10^{12}$ - $10^{17}$  GeV. One of the plausible candidates for the axionic curvaton is an imaginary component of a modulus field with mass of order 10-100 TeV and decay constant of  $10^{16}$ - $10^{17}$  GeV. We also discuss extreme cases where the curvaton drives a second inflation and find that  $f_{\text{NL}}$  is typically smaller compared to non-inflating cases.

---

<sup>1</sup>kawasaki@icrr.u-tokyo.ac.jp

<sup>2</sup>takeshi@cita.utoronto.ca

<sup>3</sup>fumi@tuhep.phys.tohoku.ac.jp

# Contents

<b>1</b>	<b>Introduction</b>	<b>1</b>
<b>2</b>	<b>Review of Curvatons with a General Potential</b>	<b>3</b>
2.1	Density Perturbations from Curvatons . . . . .	3
2.2	Case Study: Hilltop Curvatons . . . . .	6
<b>3</b>	<b>Axionic Curvatons</b>	<b>7</b>
3.1	Parameter Space in the Hilltop Regime . . . . .	8
3.2	Dependence on Various Parameters . . . . .	10
<b>4</b>	<b>Discussion</b>	<b>13</b>
<b>5</b>	<b>Conclusions</b>	<b>15</b>
<b>A</b>	<b>Inflating Curvatons</b>	<b>15</b>
A.1	Density Perturbations from Inflating Curvatons . . . . .	15
A.2	Inflating at the Hilltop . . . . .	19
A.3	Axionic Curvatons . . . . .	19

## 1 Introduction

Several theoretical difficulties of the standard big bang cosmology such as the horizon and flatness problems can be elegantly solved by inflation [1]. In fact, the existence of the inflationary era in the early Universe is strongly supported by the observations [2]; the density perturbations extending beyond the horizon at the last scattering surface can be interpreted as the evidence for the accelerated expansion in the past.

The study of density perturbations such as isocurvature perturbations, non-Gaussianity, tensor-mode, and their effects on the cosmic microwave background (CMB) power spectrum is a powerful diagnostic of the mechanism that laid down the primordial density fluctuations, but it is not enough at present to pin down the model. This is partly because of our ignorance of thermal history of the Universe beyond the standard big bang cosmology, especially concerning how the Universe was reheated.

Whereas one of the plausible explanations for the density perturbations is the quantum fluctuations of the inflaton from the minimalistic point of view, it may be that there are many other light scalars in nature, one of which is responsible for the observed density perturbation via the curvaton [3, 4, 5, 6] (or its variant, e.g. modulated reheating [7, 8]) mechanism. In fact, there are many moduli fields that necessarily appear at low energies through compactifications in string theory. Most of them must be stabilized in order to have a sensible low-energy theory, but some of them may remain relatively light, and therefore are a candidate for the curvaton. Interestingly, there is an argument that string theory contains a plenitude of axions, the so called “string axiverse.” [9] We shall see later that the axion is indeed a plausible candidate for the successful curvaton.<sup>4</sup>

---

<sup>4</sup> Throughout this paper the axions refer to imaginary components of moduli fields, which have a sinusoidal potential.

One of the distinguishing features of the curvaton mechanism is that it can generate the density perturbation with large non-Gaussianity. If any primordial non-Gaussianity is found by the Planck satellite, it would exclude a simple class of inflation models as the origin of the entire density perturbation, and therefore, it has a tremendous impact on our understanding of the early Universe.

Recently, the present authors studied non-Gaussianity generated by the curvaton mechanism in great detail, and developed a formalism to calculate the density perturbation for a generic curvaton potential [10]. We pointed out that the curvaton should be located at a potential with negative curvature during inflation, and in particular it must be close to the local maximum (“hilltop”) of the potential, in order to generate a red-tilted density perturbation spectrum which is strongly favored by the recent observations [2]. Interestingly, we found that, even if the curvaton dominates the Universe, the non-Gaussianity parameter  $f_{\text{NL}}$  is positive and gets enhanced logarithmically in the hilltop limit, and therefore  $f_{\text{NL}}$  of  $\mathcal{O}(10)$  is a robust prediction of the hilltop curvaton. Applying our formalism to the axionic (or pseudo-Nambu-Goldstone) curvaton with a sinusoidal potential, we found that  $f_{\text{NL}}$  can be as large as about 30, which is realized for the curvaton mass of order 10 TeV and the decay constant of order the GUT scale. In this analysis we fixed the scalar spectral index  $n_s = 0.96$  for simplicity. The mild increase of the non-Gaussianity in the hilltop limit is originated from the fact that the density perturbation generated by the curvaton is enhanced. This enhancement is due to non-uniform onset of curvaton oscillations [11, 10]. This result should be contrasted to a simple curvaton model with a quadratic potential, which predicts a negative  $f_{\text{NL}}$  of order unity in the case that it dominates the Universe.

In this paper, we extend our previous work on the non-Gaussianity generated by the axionic curvaton with the hilltop initial condition. We will discuss its dependence on the scalar spectral index, and also scan the curvaton parameters, namely, the mass and the decay constant. Interestingly, we find that  $f_{\text{NL}}$  is bounded as  $f_{\text{NL}} \lesssim 30$  for  $n_s = 0.94-0.99$ , and the maximal non-Gaussianity is realized for the curvaton mass 10 TeV and the decay constant of order the GUT scale. (If reheating happens prior to the curvaton oscillation, then the bound becomes  $f_{\text{NL}} \lesssim 40$ .) Furthermore,  $f_{\text{NL}} = 20-40$  is realized for a wide range of parameters, the curvaton mass  $m_\sigma = 10-10^6$  GeV and the decay constant  $f = 10^{12}-10^{17}$  GeV. One of the plausible candidates for such an axionic curvaton is an imaginary component of the moduli (i.e., axions) with mass of order 10-100 TeV and decay constant of  $10^{16-17}$  GeV. The moduli fields are stabilized by the non-perturbative effect and the supersymmetry (SUSY) breaking, and it is plausible that the moduli mass is closely related to the SUSY breaking scale in the visible sector. Intriguingly, such several tens TeV SUSY breaking scale is consistent with the recently discovered Higgs boson mass of 125-126 GeV [12, 13].

The rest of the paper is organized as follows. After briefly reviewing density perturbations from general curvatons in Section 2, then in Section 3 we discuss axionic curvatons in detail. We then give discussions and conclusions in Section 4 and 5, respectively.

The appendix discusses an extreme case where the curvaton drives a second inflationary period. After analytically computing density perturbations from inflating curvatons in general, we then apply the discussions to axionic curvatons. We find that the non-Gaussianity turns out to be rather small when the axionic curvaton drives a second inflation.

## 2 Review of Curvatons with a General Potential

In the curvaton mechanism, the light curvaton field acquires super-horizon field fluctuations during inflation. The density perturbations are produced in the post-inflationary era, as the curvaton oscillates and its energy density relatively grows compared to other radiation components. In this section we give a brief review of density perturbations generated by a curvaton  $\sigma$  with a generic effective potential  $V(\sigma)$ . We refer the reader to [10] for detailed derivation of the following results.

### 2.1 Density Perturbations from Curvatons

The density perturbations generated by curvatons depend on the curvaton dynamics during and after inflation. In the simple curvaton model with a quadratic potential, the curvaton dynamics is determined by the curvaton mass and the initial deviation from the origin. If the mass is much smaller than the Hubble parameter during inflation, the curvaton hardly evolves until it starts to oscillate, and the resultant density perturbation is given in a rather simple form. However this is no longer the case for a general curvaton potential. In particular, the curvature of the potential should be negative and non-negligible in order to account for the observationally favoured red-tilted perturbation spectrum, then the curvaton significantly evolves after inflation, affecting the density perturbation.

If the curvaton potential  $V(\sigma)$  has no explicit dependence on time, then the curvaton dynamics prior to the oscillation can be tracked by the attractor solution

$$\hat{c}H\dot{\sigma} = -V', \quad \text{with} \quad \hat{c} = \begin{cases} 3 & (\text{during inflation with } H \simeq \text{const.}) \\ 9/2 & (\text{matter domination}) \\ 5 & (\text{radiation domination}) \end{cases} \quad (2.1)$$

which is a good approximation while  $|V''/\hat{c}H^2| \ll 1$ . Here, a prime denotes a derivative with respect to  $\sigma$ , an overdot a time derivative, and  $H = \dot{a}/a$ . Setting the minimum of the potential about which the curvaton oscillates to  $\sigma = 0$ , the onset of the oscillation can be defined as when the time scale of the curvaton rolling becomes comparable to the Hubble time, i.e.

$$\left| \frac{\dot{\sigma}}{H\sigma} \right| = 1. \quad (2.2)$$

Then the Hubble parameter at the time is obtained as

$$H_{\text{osc}}^2 = \left| \frac{V'(\sigma_{\text{osc}})}{c\sigma_{\text{osc}}} \right|, \quad (2.3)$$

where the subscript ‘‘osc’’ denotes values at the onset of the curvaton oscillation, and  $c$  is a constant depending on whether reheating (= inflaton decay, at  $t_{\text{reh}}$ ) is earlier/later than the onset of the curvaton oscillation (corresponding to  $\hat{c}$  in the attractor (2.1) right before the oscillation):

$$c = \begin{cases} 9/2 & (t_{\text{reh}} > t_{\text{osc}}) \\ 5 & (t_{\text{reh}} < t_{\text{osc}}). \end{cases} \quad (2.4)$$

The absolute value sign in (2.3) can be removed by supposing the curvaton potential to be monotonically increasing (decreasing) for  $\sigma > (<)0$ , so that the curvaton can roll down to the origin.

Let us here summarize simplifying assumptions concerning the evolution of the energy densities of the curvaton and the inflaton. We assume the curvaton potential to be well approximated by a quadratic one around its minimum so that the curvaton oscillations are sinusoidal.<sup>5</sup> Then the curvaton energy density redshifts similarly to nonrelativistic matter after the onset of the oscillations until the curvaton decays into radiation. On the other hand, we consider the inflaton to behave as matter from the end of inflation until reheating when it decays into radiation. The energy density of the curvaton before the beginning of its oscillation is assumed to be negligibly tiny compared to the total energy of the Universe, having little effect on the expansion history.

Supposing the curvaton field fluctuations to be nearly Gaussian with  $\mathcal{P}_{\delta\sigma}(k) = (H|_{k=aH}/2\pi)^2$  at the time when the comoving wave mode  $k$  exits the horizon, then using the  $\delta\mathcal{N}$ -formalism [19, 20, 21, 22], the power spectrum of the density perturbations at the CMB scale is expressed as [10]

$$\mathcal{P}_\zeta = \left( \frac{\partial\mathcal{N}}{\partial\sigma_*} \frac{H_*}{2\pi} \right)^2, \quad (2.5)$$

with

$$\frac{\partial\mathcal{N}}{\partial\sigma_*} = \frac{r}{4+3r} (1-X(\sigma_{\text{osc}}))^{-1} \left\{ \frac{V'(\sigma_{\text{osc}})}{V(\sigma_{\text{osc}})} - \frac{3X(\sigma_{\text{osc}})}{\sigma_{\text{osc}}} \right\} \frac{V'(\sigma_{\text{osc}})}{V'(\sigma_*)}. \quad (2.6)$$

Here, the subscript  $*$  denotes values when the CMB scale exits the horizon, and  $r$  is the energy density ratio between the curvaton and radiation (which originates from the inflaton) upon curvaton decay

$$r \equiv \left. \frac{\rho_\sigma}{\rho_r} \right|_{\text{dec}}. \quad (2.7)$$

The function  $X$  denotes effects due to the non-uniform onset of the curvaton oscillations (which are absent for a purely quadratic curvaton potential), defined as follows:

$$X(\sigma_{\text{osc}}) \equiv \frac{1}{2(c-3)} \left( \frac{\sigma_{\text{osc}} V''(\sigma_{\text{osc}})}{V'(\sigma_{\text{osc}})} - 1 \right), \quad (2.8)$$

where the constant  $c$  is given in (2.4).

From the above expressions, the spectral index of the linear order perturbations follows as (note that the scale-dependence of (2.6) shows up only through  $\sigma_*$ , since  $\sigma_{\text{osc}}$  and  $r$  are independent of the comoving wave number)

$$n_s - 1 \equiv \frac{d}{d \ln k} \ln \mathcal{P}_\zeta = 2 \frac{\dot{H}_*}{H_*^2} + \frac{2}{3} \frac{V''(\sigma_*)}{H_*^2}. \quad (2.9)$$

The recent observations strongly suggest that the density perturbation power spectrum is red-tilted,  $n_s = 0.968 \pm 0.012$  [2]. This requires that the curvaton potential be tachyonic and the size of the curvature must be of order 10% of the Hubble parameter during inflation, unless the inflaton

---

<sup>5</sup>Cases with non-sinusoidal oscillations are discussed in Appendix B of [10]. We note that the oscillation of the hilltop axionic curvaton discussed later on can be treated simply as sinusoidal, since the curvaton quickly settles down to the part of its potential that is well approximated by a quadratic one. However, its cosine type potential (3.1) which is flatter than a quadratic may allow formation of oscillating inflaton condensates [14, 15, 16, 17, 18] during the initial oscillations. Here we remark that such oscillons, even if they formed, are not expected to alter the above analyses since their energy density redshifts as nonrelativistic matter, and also because their dynamics should not affect perturbations at the CMB scales that are super-horizon by the time the oscillons form.

is allowed to take super-Planckian field values, or some special configurations are arranged in the inflationary setup (cf. Footnote 8.)

Curvatons also generate local-type<sup>6</sup> bispectrum, whose amplitude is represented by the non-linearity parameter  $f_{\text{NL}}$ . This is given by

$$\begin{aligned}
f_{\text{NL}} &= \frac{5}{6} \frac{\partial^2 \mathcal{N}}{\partial \sigma_*^2} \left( \frac{\partial \mathcal{N}}{\partial \sigma_*} \right)^{-2} \\
&= \frac{40(1+r)}{3r(4+3r)} + \frac{5(4+3r)}{6r} \left\{ \frac{V'(\sigma_{\text{osc}})}{V(\sigma_{\text{osc}})} - \frac{3X(\sigma_{\text{osc}})}{\sigma_{\text{osc}}} \right\}^{-1} \left[ (1-X(\sigma_{\text{osc}}))^{-1} X'(\sigma_{\text{osc}}) \right. \\
&\quad \left. + \left\{ \frac{V'(\sigma_{\text{osc}})}{V(\sigma_{\text{osc}})} - \frac{3X(\sigma_{\text{osc}})}{\sigma_{\text{osc}}} \right\}^{-1} \left\{ \frac{V''(\sigma_{\text{osc}})}{V(\sigma_{\text{osc}})} - \frac{V'(\sigma_{\text{osc}})^2}{V(\sigma_{\text{osc}})^2} - \frac{3X'(\sigma_{\text{osc}})}{\sigma_{\text{osc}}} + \frac{3X(\sigma_{\text{osc}})}{\sigma_{\text{osc}}^2} \right\} \right. \\
&\quad \left. \left. + \frac{V''(\sigma_{\text{osc}})}{V'(\sigma_{\text{osc}})} - (1-X(\sigma_{\text{osc}})) \frac{V''(\sigma_*)}{V'(\sigma_*)} \right] . \tag{2.10}
\end{aligned}$$

A quadratic potential  $V \propto \sigma^2$  realizing  $X(\sigma_{\text{osc}}) = 0$  reproduces the known result for quadratic curvatons whose  $f_{\text{NL}}$  is determined only by  $r$ .

Let us also rewrite the energy density ratio  $r$  (2.7) in terms of the inflaton and curvaton parameters:

$$r = \text{Max.} \left[ \frac{V(\sigma_{\text{osc}})}{3M_p^2 H_{\text{osc}}^{3/2} \Gamma_{\sigma}^{1/2}} \times \text{Min.} \left( 1, \frac{\Gamma_{\phi}^{1/2}}{H_{\text{osc}}^{1/2}} \right), \left\{ \frac{V(\sigma_{\text{osc}})}{3M_p^2 H_{\text{osc}}^{3/2} \Gamma_{\sigma}^{1/2}} \times \text{Min.} \left( 1, \frac{\Gamma_{\phi}^{1/2}}{H_{\text{osc}}^{1/2}} \right) \right\}^{4/3} \right], \tag{2.11}$$

where  $M_p \simeq 2.4 \times 10^{18}$  GeV is the reduced Planck mass, and the first and second terms in the Max. parentheses correspond to the curvaton being subdominant and dominant at its decay, respectively, while the Min. parentheses are due to whether the onset of oscillation is after or before reheating.  $\Gamma_{\phi}$  and  $\Gamma_{\sigma}$  are constants that denote, respectively, the decay rates of the inflaton and the curvaton. We note that in obtaining the above results, we have adopted the sudden decay approximation where the scalar fields suddenly decay into radiation when  $H = \Gamma$ .

Finally, the curvaton field value at the onset of the oscillations  $\sigma_{\text{osc}}$  is obtained by integrating (2.1),

$$\int_{\sigma_*}^{\sigma_{\text{osc}}} \frac{d\sigma}{V'} = -\frac{\mathcal{N}_*}{3H_{\text{inf}}^2} - \frac{1}{2c(c-3)H_{\text{osc}}^2}, \tag{2.12}$$

which can be solved for  $\sigma_{\text{osc}}$  as a function of  $\sigma_*$ .<sup>7</sup> Here,  $\mathcal{N}_*$  is the number of e-folds during inflation between the horizon exit of the CMB scale and the end of inflation,  $c$  is given in (2.4), and  $H_{\text{inf}}$  is the inflationary Hubble scale (we are assuming a nearly constant Hubble parameter during inflation, thus  $H_{\text{inf}} \simeq H_*$ ).

<sup>6</sup>Strictly speaking, bispectra from curvatons have shapes similar to, but may not exactly be of the ‘‘local form’’ [23], especially when  $f_{\text{NL}}$  is strongly scale-dependent [24, 25, 26]. However we note that for axionic curvatons with sinusoidal potentials, the running of  $f_{\text{NL}}$  is tied to the running of the spectral index, and thus strictly constrained to be small by current observations [26].

<sup>7</sup>When (2.12) admits as solutions for  $\sigma_{\text{osc}}$  both positive and negative values, one should take the sign of  $\sigma_{\text{osc}}$  to match with that of  $\sigma_*$ .

Therefore by combining the above expressions, one can compute the density perturbations from a curvaton with a generic potential  $V(\sigma)$ , given the curvaton field value at the CMB scale horizon exit  $\sigma_*$ , the decay rates of the inflaton  $\Gamma_\phi$  and curvaton  $\Gamma_\sigma$ , the inflationary scale  $H_{\text{inf}}$ , and the duration of inflation  $\mathcal{N}_*$ .

## 2.2 Case Study: Hilltop Curvatons

As an example that will be relevant for analyzing axionic curvatons in the next section, here let us apply the above generic results to a curvaton located at the hilltop, whose potential around  $\sigma_{\text{osc}}$  and  $\sigma_*$  is well approximated by

$$V(\sigma) = V_0 - \frac{1}{2}m^2(\sigma - \sigma_0)^2, \quad (2.13)$$

where  $m$ ,  $\sigma_0$ , and  $V_0(> 0)$  are constants. Without loss of generality, we assume  $0 < \sigma_{\text{osc}} < \sigma_* < \sigma_0$ . Then one can check that when the curvaton is close enough to the hilltop to satisfy

$$\sigma_{\text{osc}} \gg \sigma_0 - \sigma_{\text{osc}}, \quad V_0 \gg m^2(\sigma_0 - \sigma_{\text{osc}})^2, \quad (2.14)$$

then the resulting power spectrum (2.5) and the non-Gaussianity (2.10) take the form

$$\mathcal{P}_\zeta^{1/2} \simeq \frac{3r}{4 + 3r} \frac{\sigma_0 - \sigma_{\text{osc}}}{\sigma_0 - \sigma_*} \frac{H_*}{2\pi\sigma_{\text{osc}}}, \quad (2.15)$$

$$f_{\text{NL}} \simeq \frac{5(4 + 3r)}{18r} \frac{\sigma_{\text{osc}}}{\sigma_0 - \sigma_{\text{osc}}}, \quad (2.16)$$

with spectral index (2.9)

$$n_s - 1 = 2 \frac{\dot{H}_*}{H_*^2} - \frac{2}{3} \frac{m^2}{H_*^2}. \quad (2.17)$$

The equation (2.12) which relates  $\sigma_*$  and  $\sigma_{\text{osc}}$  gives

$$\ln \left( \frac{\sigma_0 - \sigma_*}{\sigma_0 - \sigma_{\text{osc}}} \right) \simeq -\frac{1}{2(c-3)} \frac{\sigma_{\text{osc}}}{\sigma_0 - \sigma_{\text{osc}}}, \quad (2.18)$$

where we dropped the  $H_{\text{inf}}^2$  contribution on the right hand side from the condition (2.14) and also by assuming  $m^2/H_{\text{inf}}^2 \lesssim 10^{-2}$ . As the initial value  $\sigma_*$  is shifted towards the hilltop,  $\sigma_{\text{osc}}$  approaches  $\sigma_0$  much slower than  $\sigma_*$  does since the left hand side is logarithmic. Therefore as one approaches the hilltop,  $\mathcal{P}_\zeta$  (2.15) blows up due to the enhancement factor  $(\sigma_0 - \sigma_{\text{osc}})/(\sigma_0 - \sigma_*)$ , while  $f_{\text{NL}}$  (2.16) increases slowly. We also note that the value of  $f_{\text{NL}}$  is greater than one even when  $r \gg 1$ , from (2.14). The extreme amplification of the linear perturbations corresponds to the curvaton taking longer time to start its oscillation when starting closer to the hilltop.

Before ending this section, we should remark that in the extreme hilltop limit, the approximation (2.1) for the curvaton dynamics mildly breaks down before the curvaton starts to oscillate. This gives rise to errors of  $\mathcal{O}(1)$  for the above results in this limit. However, the above analytic expressions suffice for our order of magnitude estimations on axionic curvatons in the next section. We will also carry out numerical computations when further accuracy is required, e.g., when calculating predictions on  $f_{\text{NL}}$ .

### 3 Axionic Curvatons

Now let us move on to the investigation of axionic curvatons, which is the main topic of this paper. As was explained in the introduction, we focus on the case where the curvaton is a pseudo-Nambu-Goldstone boson of a broken U(1) symmetry, possessing a periodic potential of the form

$$V(\sigma) = \Lambda^4 \left[ 1 - \cos \left( \frac{\sigma}{f} \right) \right], \quad (3.1)$$

where  $f$  and  $\Lambda$  are mass scales. Without loss of generality, we restrict the initial field value to lie within the range  $0 < \sigma_* < \pi f$ . The curvaton's effective mass at the potential minimum is denoted by

$$m_\sigma = \frac{\Lambda^2}{f}. \quad (3.2)$$

Then supposing that the coupling of the axionic curvaton with its decay product is suppressed by the symmetry breaking scale  $f$ , the curvaton decay rate takes the value

$$\Gamma_\sigma = \frac{\beta}{16\pi} \frac{m_\sigma^3}{f^2} = \frac{\beta}{16\pi} \frac{\Lambda^6}{f^5}, \quad (3.3)$$

where the constant  $\beta$  is naively of order unity. In the following, we ignore the time-variation of the Hubble parameter during inflation, and especially, neglect the  $\dot{H}$  contribution to the spectral index (2.9). In other words, we do not consider inflationary models with rather large  $|\dot{H}/H^2|$  which requires super-Planckian field ranges or some special configurations.<sup>8</sup> Hence the axionic curvaton need to be located beyond the inflection point during inflation, i.e.  $0.5 < \sigma_*/\pi f < 1$ , in order to source a red-tilted power spectrum.

The axionic curvaton with  $\sigma_* \ll \pi f$  whose potential is well approximated by a quadratic was studied in [29], and the whole potential including the hilltop region was investigated in [10]. There it was shown along the line of discussion in Section 2.2, that unless the axionic curvaton is initially located close to the hilltop, both the inflation and reheating scales need to be very high. For e.g., for  $\sigma_*/\pi f = 0.75$  to satisfy both the WMAP normalization  $P_\zeta \approx 2.42 \times 10^{-9}$  and the spectral index  $n_s \approx 0.96$ , then  $H_{\text{inf}} \gtrsim 10^{13}$  GeV and  $\rho_{\text{reh}}^{1/4} \gtrsim 10^{13}$  GeV are required, where  $\rho_{\text{reh}}$  represents the radiation energy density at the reheating. This is because the spectral index of order  $1 - n_s \sim 0.01$  requires a rather large curvaton mass  $m_\sigma \sim 0.1 H_{\text{inf}}$ , forcing the curvaton to start its oscillation soon after the end of inflation. Hence without high inflation and reheating scales, the curvaton cannot even come close to dominating the Universe to source measurable density perturbations.<sup>9</sup> The story

<sup>8</sup>Assuming single-field canonical slow-roll inflation, the Lyth bound [27] relates the time-variation of the Hubble parameter with the inflaton field  $\phi$  range as

$$\frac{1}{M_p^2} \left( \frac{d\phi}{d\mathcal{N}} \right)^2 \simeq -2 \frac{\dot{H}}{H^2},$$

where  $M_p$  is the reduced Planck mass and  $\mathcal{N}$  the e-folding number. Thus  $|\dot{H}/H^2|$  as large as to give sizable contribution to the spectral index (2.9) whose typical value is  $n_s \approx 0.968$  (WMAP central value) normally requires a super-Planckian field range for the inflaton. The field range bound may be alleviated by inflaton potentials giving sudden changes to  $d\phi/d\mathcal{N}$  during inflation [28].

<sup>9</sup>The curvaton's effective mass during inflation is decoupled from the mass at the potential minimum (3.2) when the curvaton is close to the inflection point, i.e.  $\sigma_*/\pi f \approx 0.5$ , however in such case even higher inflation/reheating scales are required.



is quite different for an axionic curvaton in the hilltop region, where the onset of the oscillation is delayed and curvaton domination is allowed with lower inflation/reheating scales. This, together with the amplification of the linear perturbations in the hilltop limit (cf. discussions around (2.18)), makes axionic curvatons compatible with many orders of magnitude of the inflation and reheating scales.

In light of the above considerations, in this section we elaborate on axionic curvatons in the hilltop region, which dominate the Universe before decaying into radiation. We will find that this particular limit of axionic curvatons has interesting predictions, especially in terms of the non-Gaussianity.

### 3.1 Parameter Space in the Hilltop Regime

The axionic curvaton model has five free parameters, which are the symmetry breaking scale  $f$ , the effective mass  $m_\sigma = \Lambda^2/f$ , the curvaton field value at CMB scale horizon exit  $\sigma_*$ , the inflationary scale  $H_{\text{inf}}$ , and the inflaton decay rate  $\Gamma_\sigma$ . However, since we are focusing on a curvaton that dominates the Universe before it decays, as long as there exists a parameter window which allows  $r \gg 1$ , the cosmological observables do not depend on the explicit value of  $r$  or  $\Gamma_\sigma$ . In this sense, the dominant axionic curvaton is actually a four parameter model.

Strictly speaking, there are three more parameters: the e-folding number  $\mathcal{N}_*$  between the CMB scale horizon exit and the end of inflation, the constant  $c$  (2.4) representing whether  $t_{\text{reh}} \gtrless t_{\text{osc}}$  (though this is determined when the other parameters such as  $\Gamma_\phi$  are fully given), and  $\beta$  in (3.3) parameterizing the curvaton decay rate.  $\mathcal{N}_*$  determines how much the curvaton rolls during inflation (cf. (2.12)), however such rolling is negligible compared to that in the post-inflationary era as seen in (2.18), and thus has little effects on the model. Hence we simply fix the e-folding number to  $\mathcal{N}_* = 50$  in the following discussions. As for  $c$ , whether reheating happens before/after the onset of the curvaton oscillations do not affect the allowed parameter window for  $f$  and  $m_\sigma$ , but give slightly different predictions on  $f_{\text{NL}}$ . This will be discussed in Section 3.2. The parameter  $\beta$  for the decay rate is set to unity in the following, and implications of  $\beta$  taking other values are also discussed later.

Out of the four parameters,  $H_{\text{inf}}$  and  $\sigma_*/f$  can be fixed from the WMAP normalization

$$\mathcal{P}_\zeta \approx 2.4 \times 10^{-9}, \quad (3.4)$$

and also from requiring the spectral index to be consistent with the WMAP bound

$$n_s \approx 0.96. \quad (3.5)$$

Later on we will see that the detailed value of the spectral index, as long it is not so close to unity, only have minor effects on axionic curvatons. Hence we are left with two parameters for the axionic curvaton  $f$  and  $m_\sigma$ . Order of magnitude constraints on these parameters can be obtained using the analytic formulae in Section 2 (or in Section 2.2), which we present in Figure 1. The yellow region corresponds to the allowed window for a dominant axionic curvaton in the hilltop.  $H_{\text{inf}}$  and  $\sigma_*/f$  are fixed to appropriate values by the observational constraints (3.4) and (3.5) at each point in the window, as indicated in the upper figures showing their contour lines. This also fixes the curvaton decay rate via (3.3), cf. lower left figure. (The relativistic degrees of freedom is fixed to  $g_* = 100$

upon drawing the  $T_{\text{dec}}$  contours). On the other hand, the inflaton decay rate  $\Gamma_\phi$  is not fixed at each point but is allowed to take values within a certain range, as we will soon explain. The lower right figure shows contour lines for the non-Gaussianity  $f_{\text{NL}}$ , which is typically a few tens. Here we note that since the analytic formulae in the previous section can contain  $\mathcal{O}(1)$  errors (cf. discussions at the end of Section 2.2), the  $f_{\text{NL}}$  values have been computed numerically. We have shown the  $f_{\text{NL}}$  contours inside the allowed window where the constraints described in the following are well satisfied, but the values can be modified at regions very close to the boundaries.

We find that the allowed window is constrained by the following four conditions: The upper edge (green line) is set by the requirement that the curvaton initially lies in the hilltop regime,

$$\frac{\sigma_*}{\pi f} > 0.9. \quad (3.6)$$

Recall that a non-hilltop axionic curvaton can work only with very high inflation/reheating scales. The right edge (blue line) denotes the requirement that the curvaton be subdominant until it starts its oscillation,

$$V(\sigma_{\text{osc}}) < 0.1 \times 3M_p^2 H_{\text{osc}}^2. \quad (3.7)$$

When going beyond this boundary, the curvaton starts to drive a secondary inflation. A rather strict relationship between  $H_{\text{in}}$  and  $\sigma_*/f$  is required for such inflating curvatons to work, as is discussed in Appendix A. The lower edge (orange line) requires the curvaton to decay at temperatures higher than 5 MeV in order not to ruin Big Bang Nucleosynthesis (BBN) [30, 31, 32, 33], i.e.

$$3M_p^2 \Gamma_\sigma^2 > \frac{\pi^2}{30} g_*(5 \text{ MeV})^4, \quad (3.8)$$

with the relativistic degrees of freedom  $g_* = 10.75$ . Finally, the left edge (red line) follows from the dominant condition <sup>10</sup>

$$r > 10. \quad (3.9)$$

These conditions give the most stringent constraints on the hilltop axionic curvaton, and other requirements for a consistent curvaton scenario are satisfied in the window bordered by (3.6) - (3.9).

Let us also lay out such satisfied conditions: Firstly, the curvaton energy density is negligibly small during inflation,

$$V(\sigma_*) \ll 3M_p^2 H_{\text{inf}}^2. \quad (3.10)$$

Moreover, quantum fluctuations during inflation should not make the curvaton jump over its potential minimum in order to avoid the resulting density perturbations from being highly non-Gaussian, or over the maximum to avoid domain walls,

$$\frac{H_{\text{inf}}}{2\pi} \ll \sigma_* \ll \pi f - \frac{H_{\text{inf}}}{2\pi}. \quad (3.11)$$

In the hilltop region, the classical rolling becomes suppressed, which can compete with the quantum fluctuations during inflation.<sup>11</sup> The curvaton's classical rolling dominates over the quantum

<sup>10</sup> If the curvaton is subdominant at the decay, namely,  $r \ll 1$ , the non-Gaussianity tends to be too large, and one has to tune the decay rates of the curvaton and the inflaton so that  $r \gtrsim 0.01$  is realized in order to be consistent with the observations. We have nothing new to add to this possibility in our context.

<sup>11</sup>The randomized case of axionic curvatons at the potential minimum is discussed in [29].

fluctuations if

$$\frac{3}{2\pi} \frac{H_{\text{inf}}^3}{V'(\sigma_*)} \ll 1, \quad (3.12)$$

where the curvaton is considered to slow-roll due to (3.10) and the lightness condition that follows from the spectral index (3.5). Furthermore, the curvaton decay should happen after reheating and the onset of the oscillations,

$$\Gamma_\sigma < \Gamma_\phi, H_{\text{osc}}. \quad (3.13)$$

The mass  $m_\sigma$  is required to be larger than the curvaton decay temperature, in order to avoid possible backreaction effects to the curvaton's perturbative decay (see e.g. [34, 35, 36]). Assuming instant thermalization, this condition is written roughly as

$$m_\sigma^2 > (3M_p^2 \Gamma_\sigma^2)^{1/2}. \quad (3.14)$$

As for the inflaton sector, the energy scale of reheating (= inflaton decay) is lower than that of inflation, while an upper bound on the inflationary scale is given by constraints on primordial gravitational waves. The 7-year WMAP+BAO+ $H_0$  gives  $\mathcal{P}_T/\mathcal{P}_\zeta < 0.24$  (95% CL), which translates into<sup>12</sup>

$$\Gamma_\phi < H_{\text{inf}} < 1.3 \times 10^{14} \text{ GeV}. \quad (3.15)$$

Let us repeat that all the requirements (3.10) - (3.15) are satisfied in the allowed window of Figure 1.

We should also remark on the constraints on the reheating scale  $\Gamma_\phi$  before ending this subsection. As we have noted above, dominant axionic curvatons are insensitive to the explicit value of  $\Gamma_\phi$ . The only constraints on  $\Gamma_\phi$  are that the inflaton should decay after the end of inflation (3.15) but before the curvaton decay (3.13). For the case of  $t_{\text{osc}} < t_{\text{reh}}$ , the dominant condition (3.9) sets an additional lower bound on  $\Gamma_\phi$ , cf. (2.11).<sup>13</sup> The inflaton decay rate should take values within these bounds at each point of the allowed window in Figure 1. We note that the contour lines of various quantities in the figures are obtained assuming that the values of  $\Gamma_\phi$  at each point do not saturate the lower/upper bounds set by the above requirements. If, for example,  $\Gamma_\phi$  takes lowest possible values saturating the dominant condition (3.9) for the  $t_{\text{osc}} < t_{\text{reh}}$  case, then  $r$  becomes as small as  $\approx 10$ , slightly modifying  $f_{\text{NL}}$  from the shown values.

### 3.2 Dependence on Various Parameters

The spectral index  $n_s - 1 = -2m_\sigma^2/3H_{\text{inf}}^2$  fixes the inflationary scale  $H_{\text{inf}}$  proportional to the curvaton mass  $m_\sigma$ , as is shown in the upper right figure. The rather wide range allowed for  $m_\sigma$  is translated into the axionic curvaton being compatible with inflationary scales with many orders of magnitude.

<sup>12</sup>When the inflation scale is high enough to saturate the bound (3.15), then depending on the inflationary mechanism, one can expect to have a contribution to the spectral index from a non-vanishing  $\dot{H}/H^2$  (see also Footnote 8), as well as the central value of the spectral index bounds (3.5) being slightly shifted. We ignore such effects for axionic curvatons, since they can modify the results only at the vicinity of the upper right corner of the allowed window in Figure 1.

<sup>13</sup>For the case of  $t_{\text{osc}} < t_{\text{reh}}$ , the left red edge actually denotes where the upper bound on  $\Gamma_\phi$  set by  $\Gamma_\phi < H_{\text{osc}}$  and the lower bound from the dominant condition (3.9) take the same values. In other words,  $t_{\text{osc}} < t_{\text{reh}}$  and (3.9) are incompatible beyond the red line. On the other hand, for the  $t_{\text{osc}} > t_{\text{reh}}$  case,  $r$  is independent of  $\Gamma_\phi$ , which allows one to set the dominant condition (3.9) independently of  $\Gamma_\phi$ . However we note that (3.9) produces the left red edge at the same place on the  $f - m_\sigma$  plane for both  $t_{\text{reh}} \gtrless t_{\text{osc}}$  cases.

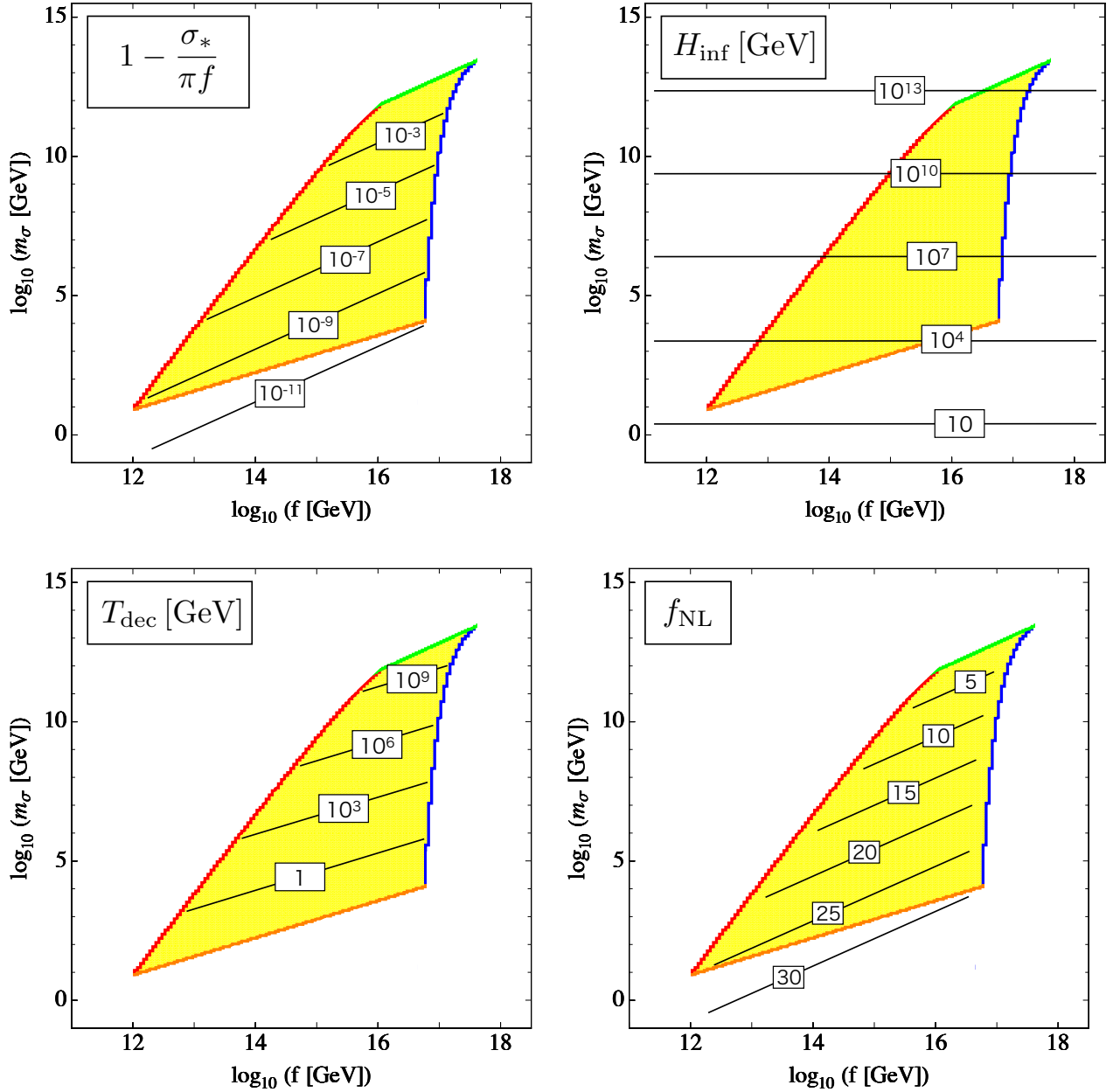


Figure 1: Parameter space for a dominant axionic curvaton in the hilltop. The allowed window is shown as the yellow region, which is bordered by the hilltop condition (3.6) (upper green boundary), the requirement that the curvaton does not inflate the Universe (3.7) (right blue), BBN constraint (3.8) (lower orange), and the dominant condition (3.9) (left red). These conditions have been adopted in order to study the peculiar behavior of the hilltop curvaton. However the curvaton mechanism can still work when relaxing some of them, see the discussions in Appendix A and footnote 10. The contour lines on each figure denote the following quantities. Upper left: The curvaton value at CMB scale horizon exit  $(\pi f - \sigma_*)/\pi f$ . Upper right: Inflationary scale  $H_{\text{inf}}$  in units of GeV. Lower left: Decay temperature  $T_{\text{dec}}$  of the curvaton in units of GeV. Lower right: Non-Gaussianity  $f_{\text{NL}}$  for the case of  $t_{\text{osc}} < t_{\text{reh}}$ . The values of  $f_{\text{NL}}$  slightly increases when  $t_{\text{osc}} > t_{\text{reh}}$ .

The upper left figure shows the curvaton's initial value  $\sigma_*$ , which comes closer to the hilltop  $\pi f$  towards the lower right corner of the allowed region. However when so close to the hilltop such that  $\sigma_*/\pi f \gtrsim 1 - 10^{-11}$ , then the axionic curvaton either ruins BBN, or drives a secondary inflation. For dominant curvatons  $r \gg 1$ , the non-Gaussianity  $f_{\text{NL}}$  is determined by how close the curvaton initially is to the hilltop (cf. (2.16) and (2.18)), thus the  $f_{\text{NL}}$  contours run parallel to those of  $(\pi f - \sigma_*)/\pi f$ . Here, recall that when shifting  $\sigma_*$  towards the hilltop,  $\sigma_{\text{osc}}$  increases much slower than  $\sigma_*$  does. This leads to a mild increase of  $f_{\text{NL}}$ , whose largest possible value is  $\sim 30$  for the case of  $t_{\text{osc}} < t_{\text{reh}}$ , and  $\sim 40$  for  $t_{\text{osc}} > t_{\text{reh}}$ . We also note that the regime beyond the right blue edge corresponds to axionic curvatons driving a second inflationary stage. However, such inflating axionic curvatons produce rather small non-Gaussianity, as discussed in detail in Appendix A.

Now let us discuss the model dependence on other parameters.

### Reheating Before/During Curvaton Oscillations

Whether reheating happens before or during the curvaton oscillation only slightly modify the curvaton velocity prior to the oscillation. This does not affect our order of magnitude estimation on the allowed window in the  $f - m_\sigma$  plane, except for that the case of  $t_{\text{reh}} < t_{\text{osc}}$  restricts the inflaton decay rate  $\Gamma_\phi$  to lie within a rather narrow range [10]. The  $\sigma_*/\pi f$ ,  $H_{\text{inf}}$ , and  $T_{\text{dec}}$  contours are also nearly the same for the two cases, however we note that  $f_{\text{NL}}$  can be slightly larger when  $t_{\text{reh}} < t_{\text{osc}}$ . This is because a radiation dominated Universe allows  $\sigma$  to roll less compared to when dominated by matter, and thus slightly makes  $\sigma_{\text{osc}}$  closer to the hilltop. The lower right figure shows the  $f_{\text{NL}}$  contours for  $t_{\text{reh}} > t_{\text{osc}}$ , but the case of  $t_{\text{reh}} < t_{\text{osc}}$  increases the  $f_{\text{NL}}$  values by up to  $\sim 10$ .

### Spectral Index

The allowed window and non-Gaussianity are insensitive to the explicit value of  $n_s$  (whether  $n_s$  is, say, 0.94 or 0.98). However, if the spectral index is as close to unity as  $n_s > 0.99$ , then the curvaton potential is required to be so flat such that the quantum fluctuations can dominate over the curvaton's classical rolling during inflation in the hilltop regime. When increasing  $n_s$  beyond 0.99 towards unity, the condition (3.12) is violated first in the lower right corner of the allowed window in the  $f - m_\sigma$  plane, and eventually in the entire window at  $n_s \gtrsim 0.999$ . Normally the model loses precise predictions if the quantum fluctuations dominate over the classical rolling. However we expect that the predictions for hilltop curvatons are not affected much by such quantum jumps during inflation, since it is the non-uniform onset of the curvaton oscillation that mainly generates the linear and second order perturbations, and also because (3.11) is satisfied even for  $n_s \approx 0.999$ , i.e., the quantum jumps (even when they dominate the curvaton dynamics) do not drastically change the curvaton position during inflation. We leave this question for future work, and let us close this paragraph by stating that as long as  $n_s \lesssim 0.99$ , the detailed values of the spectral index has little effect on axionic curvatons.

### Curvaton Decay Rate

We have been setting  $\beta$  as unity in the curvaton decay rate (3.3). A further suppressed  $\Gamma_\sigma$  (i.e. smaller  $\beta$ ) delays the curvaton decay, thus makes the BBN constraint (3.8) more stringent, while

making it easier for the curvaton to dominate the Universe and relaxes the dominant condition (3.9). For example,  $\beta = 10^{-3}$  tightens the lower edge (orange boundary) of the allowed window in Figure 1 by  $\Delta(\log_{10} m_\sigma) \sim 1$ , but pushes out the left edge (red) slightly (i.e. does not change the order of  $f$ ). It should be noted that the tightening of the BBN constraint results in decreasing the largest possible value for  $f_{\text{NL}}$ , as can be seen in the lower figure. For  $\beta = 10^{-3}$ , the maximum  $f_{\text{NL}}$  is about 27.

## 4 Discussion

The upshot of our results is that an axionic curvaton generating density perturbations consistent with current observations also generically produce non-Gaussianity  $f_{\text{NL}}$  of  $\mathcal{O}(10)$ , even when the curvaton dominates the Universe. In particular, as one can see from Fig. 1,  $f_{\text{NL}} = 20$ -40 is realized for the curvaton mass  $m_\sigma = 10$ - $10^6$  GeV and the decay constant  $f = 10^{12}$ - $10^{17}$  GeV.

What is the plausible candidate for the axionic curvaton? Interestingly, there are many moduli fields ( $T$ ) in the string theory, and they are massless at the perturbative level because of the shift symmetry,

$$T \rightarrow T + i\alpha, \quad (4.1)$$

where  $\alpha$  is a real transformation parameter. After the moduli fields are stabilized by non-perturbative effects and SUSY breaking, the imaginary components of the moduli fields, namely the (string) axions, acquire a sinusoidal potential like Eq. (3.1). The symmetry breaking scale  $f$  is naively expected to be of order the GUT or Planck scale. Thus, the string axion is one of the plausible candidates for the axionic curvatons.<sup>14</sup>

Recently, the standard-model like Higgs boson was discovered by the ATLAS and CMS experiments [12, 13]. The observed Higgs boson mass is about 125-126 GeV, which can be explained if SUSY is realized at a relatively high scale [37, 38], ranging from 10 TeV up to several tens PeV depending on the ratio of the up- and down-type Higgs boson VEVs. While the axion mass crucially depends on the stabilization mechanism, it is related to the gravitino mass in a KKLT-type stabilization [39], and so, it is conceivable that the axion mass is not many orders of magnitude different from the suggested SUSY breaking scale in the visible sector. It is intriguing that the axion with mass of this order can generate a large non-Gaussianity within the reach of the Planck satellite.

The initial position of the curvaton must be very close to the hilltop of the potential. If some symmetries are restored at the maximum of the potential, the curvaton sits initially very close to the hilltop without any fine-tuning. This is possible if one considers a moduli space spanned by multiple scalar fields [40]. To be concrete, we consider a supersymmetric theory with the superpotential,

$$W = S(\mu^2 - \chi^2 - \phi^2). \quad (4.2)$$

Here  $S$ ,  $\chi$  and  $\phi$  are chiral superfields, and  $\mu$  is a mass scale that is real. We assume that both  $\chi$  and  $\phi$  parameterize D-flat directions so that their origins are enhanced symmetry points where the corresponding gauge fields become massless. In the supersymmetric limit, there is a moduli space characterized by

$$\chi^2 + \phi^2 = \mu^2, \quad (4.3)$$

---

<sup>14</sup> The real component may play a role of the inflaton, in which case the moduli explains both the inflation and the origin of density perturbations.

where it should be noted that both  $\chi$  and  $\phi$  are complex scalar fields. The scalar potential vanishes in the moduli space. There are two special symmetry-enhanced points, i.e.,  $\chi = 0$  and  $\phi = 0$ . The degrees of freedom orthogonal to the moduli space are heavy, and can be integrated out. For instance,  $\chi$  is heavy at  $\phi \approx 0$ , one of the symmetry enhanced points, and we can erase  $\chi$  by using (4.3). In order to see that the potential has extrema at those symmetry enhanced points, let us introduce a soft SUSY breaking mass,  $m^2|\chi|^2$ , which lifts the moduli space. A similar soft SUSY breaking mass can be introduced for  $\phi$ , but it does not change the argument. Since it is  $\phi$  that is light at  $\phi \approx 0$ , the effective potential can be written as

$$V_{\text{eff}} = m^2|\mu^2 - \varphi^2|, \quad (4.4)$$

where we have supposed  $m^2 > 0$  and minimized the angular component of  $\phi$ , and defined  $\varphi \equiv |\phi|$ . Thus,  $\phi = 0$  is the local maximum. Note that one should write the effective potential in terms of  $\chi$  at  $\varphi \approx \mu$ , since  $\phi$  becomes heavy and it is  $\chi$  that is light. Then the potential is simply given by  $m^2|\chi|^2$ , which clearly shows that the potential is minimized at  $\chi = 0$  (or  $\varphi = \mu$ ).

Now let us discuss other cosmological issues. In order to have successful cosmology, it is necessary to generate a right amount of baryon asymmetry and dark matter. Since the baryonic/CDM isocurvature density perturbation is tightly constrained by observations, it also limits possible baryogenesis and dark matter candidates [41]. If the baryon asymmetry is generated (or dark matter density is fixed) before the curvaton dominates the Universe, too large isocurvature perturbation will be produced. Thus, both baryon asymmetry and dark matter must be generated after the curvaton domination. The Hubble parameter at the curvaton domination  $H_{\text{dom}}$  depends on the reheating temperature as well as on the curvaton parameters, hence the value of  $H_{\text{dom}}$  is not uniquely determined at each point in Figure 1. Largest values for  $H_{\text{dom}}$  at each point are realized when  $t_{\text{reh}} \leq t_{\text{osc}}$ ,<sup>15</sup> in such case  $H_{\text{dom}}$  increases as  $m_\sigma$  and  $f$ . For  $m_\sigma = 10 \text{ TeV} - 100 \text{ PeV}$  and  $f \sim 10^{17} \text{ GeV}$ , it ranges from 10 GeV to 100 TeV. There are several baryogenesis mechanisms which work at a Hubble parameter below  $H_{\text{dom}}$ . For instance, in the Affleck-Dine mechanism [42, 43], the baryon number is generated and fixed when the Hubble parameter is comparable to the soft mass of the flat direction in the MSSM. For the sfermion masses of order 10-100 TeV, it is possible that the AD field starts to oscillate after the curvaton domination. Since the mass of the AD field at large field value has rather large uncertainty,  $H_{\text{dom}}$  below TeV may be also allowed; for instance, this is the case if the potential of the AD field becomes flatter at large fields values. There are many dark matter candidates. Since the curvaton decays just before BBN for the case of our interest, there is an entropy dilution. One of the plausible dark matter candidates is the QCD axion, which starts to oscillate when the plasma temperature drops down to the QCD scale. There may be other ultralight axions which contribute to the dark matter density. Also, the thermal relic abundance of the WIMPs as well as WIMPs non-thermally produced by the curvaton decays are candidates for the dark matter.

We have assumed that the curvaton is responsible for the observed density perturbation. From the minimalistic point of view, of course, the quantum fluctuation of the inflaton is the leading candidate. However, requiring both an extremely flat potential for sufficiently long inflation and the normalization of density perturbation may be too strong constraint on the inflation sector. If there are many other light scalars in nature, it might be more probable that there are two scalars, namely,

---

<sup>15</sup>One can check that  $H_{\text{dom}}$  becomes independent of the reheating temperature when  $t_{\text{reh}} \leq t_{\text{osc}}$ .

the inflaton and the curvaton, responsible for the inflationary expansion and the origin of density perturbations, respectively.

## 5 Conclusions

In this paper we have studied non-Gaussianity of the density perturbation generated by the axionic curvaton, focusing on the case that the curvaton initially sits near the hilltop of the potential during inflation, and dominates the Universe before it decays. Interestingly, we have found that the non-Gaussianity parameter  $f_{\text{NL}}$  is positive and gets enhanced up to 30 (or 40 for early reheating) in the hilltop limit, even when the curvaton dominates the Universe. We have confirmed that this conclusion holds for  $n_s = 0.94-0.99$ . It was also shown that in extreme cases where the axionic curvaton drives a secondary inflation, then the produced non-Gaussianity is typically  $f_{\text{NL}} \lesssim 10$  and is smaller than non-inflating cases. Note that, as long as the curvaton dominates the Universe,  $f_{\text{NL}}$  cannot be larger than 30-40; this should be contrasted to other scenarios which can generate arbitrarily large non-Gaussianity, and some parameters must be tuned to realize  $f_{\text{NL}} = \mathcal{O}(10)$ . We have also pointed out that one of the plausible candidates for the axionic curvaton is the string axion with mass of order 10-100 TeV and decay constant of  $10^{16-17}$  GeV. If there are many axions in the Universe, one of them may be indeed responsible for the origin of the density perturbation.

## Acknowledgements

This work was supported by the Grant-in-Aid for Scientific Research on Innovative Areas (No.24111702[FT], No. 21111006[FT,MK], and No.23104008[FT]), Scientific Research (A) (No. 22244030 and No.21244033 [FT]), Scientific Research (C) (No. 14102004 [MK]) and JSPS Grant-in-Aid for Young Scientists (B) (No. 24740135) [FT]. This work was also supported by World Premier International Center Initiative (WPI Program), MEXT, Japan.

## A Inflating Curvatons

In this appendix we consider the possibility that the curvaton drives a second inflationary stage before it starts to oscillate. After giving general discussions on density perturbations sourced by such inflating curvatons, we study the case for axionic curvatons.

### A.1 Density Perturbations from Inflating Curvatons

The case studied in this appendix is illustrated in Figure 2: The curvaton initially (i.e. during the first inflationary era) has negligibly tiny energy density compared to the total energy, however dominates the universe before it starts its oscillation. We suppose that this second inflationary period is not so long, and the CMB scale exits the horizon during the first inflation. The curvaton's field fluctuations obtained from the first inflation lead to slight difference in the lengths of the second inflationary periods among different patches of the universe, thus generate the density perturbations.



We also note that the second inflation is not necessarily a slow-roll one, but may be a rapid-roll inflation [44, 45, 46, 47, 48], depending on the curvaton potential.<sup>16</sup>

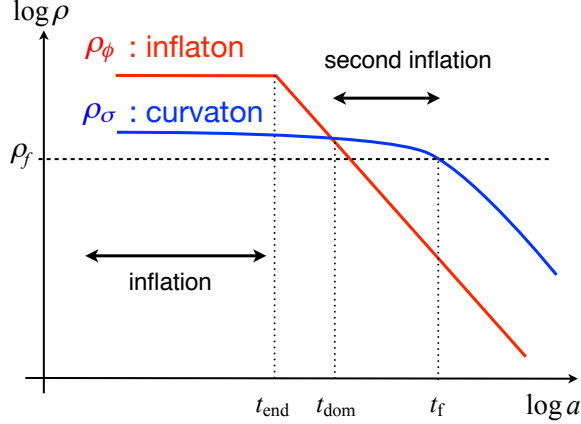


Figure 2: Schematic of the time variation of energy densities in an inflating curvaton scenario.

Upon calculating the density perturbations using the  $\delta\mathcal{N}$ -formalism, we assume that the second inflation lasts long enough (say, more than one e-fold) such that during this period the inflaton energy density becomes negligibly tiny and then the universe is well described as composed only of the curvaton. This assumption allows us to choose the final uniform energy hypersurface to possess energy density  $\rho_f$  equal to or larger than that at the end of the second inflationary period, cf. Figure 2. In other words, we set the final hypersurface to be before the end of the curvaton-driven inflation, but late enough so that after which the inflaton can be ignored and no further  $\delta\mathcal{N}$  is produced.

The energy density of the inflaton  $\phi$  is considered to redshift as  $\rho_\phi \propto a^{-3}$  after the first inflation, and we first study the case where the inflaton decay happens after the curvaton domination. Moreover, the curvaton  $\sigma$  is assumed to drive slow/rapid-roll inflation after dominating the universe. Hereafter we use the subscripts  $*$  to denote values when the CMB scale exits the horizon (during the first inflation), “end” for values at the end of inflation, “dom” for when the curvaton starts to dominate the universe (i.e.  $\rho_{\phi \text{ dom}} = \rho_{\sigma \text{ dom}}$ ), and “f” at the final constant energy density hypersurface. Then in order to compute the resulting density perturbations, we would like to obtain the  $\sigma_*$ -dependence of the e-folding number from the end of inflation until the final surface ( $\rho_\sigma$  is negligibly tiny during the first inflation, thus the curvaton has little effect on the expansion history before  $t_{\text{end}}$ ):

$$\mathcal{N} = \mathcal{N}_a + \mathcal{N}_b, \quad (\text{A.1})$$

where

$$\mathcal{N}_a \equiv \int_{t_{\text{end}}}^{t_{\text{dom}}} H dt, \quad \mathcal{N}_b \equiv \int_{t_{\text{dom}}}^{t_f} H dt. \quad (\text{A.2})$$

Here  $H = \dot{a}/a$ , with an overdot denoting a time-derivative.

<sup>16</sup>Note that the curvaton field fluctuations at the CMB scale is generated during the first inflation, thus the resulting density perturbations can be (nearly) scale-invariant even if the second inflation is a rapid-roll one.

We take  $V(\sigma)$  to be the energy potential of the curvaton, which we assume to have no explicit time dependence. Then using  $\rho_{\sigma_{\text{dom}}} \simeq V(\sigma_{\text{dom}})$ , one finds

$$\mathcal{N}_a = \frac{1}{3} \ln \frac{\rho_{\phi_{\text{end}}}}{\rho_{\phi_{\text{dom}}}} \simeq \frac{1}{3} \ln \frac{\rho_{\phi_{\text{end}}}}{V(\sigma_{\text{dom}})}, \quad (\text{A.3})$$

thus

$$\frac{\partial \mathcal{N}_a}{\partial \sigma_*} \simeq -\frac{1}{3} \frac{V'(\sigma_{\text{dom}})}{V(\sigma_{\text{dom}})} \frac{\partial \sigma_{\text{dom}}}{\partial \sigma_*}, \quad (\text{A.4})$$

where a prime denotes a derivative in terms of  $\sigma$ . However, we will soon see that  $\delta \mathcal{N}_a$  only gives a minor contribution to the density perturbations.

After the curvaton domination, for simplification, we ignore  $\rho_\phi$  and describe the second inflation as a single-component slow/rapid-roll inflation.<sup>17</sup> Then the inflationary dynamics is approximated by (cf. appendix of [48]),

$$3M_p^2 H^2 \simeq V, \quad \tilde{c} H \dot{\sigma} \simeq -V', \quad \text{where } \tilde{c} = \frac{3 + \sqrt{9 - 12\eta}}{2}, \quad \eta \equiv M_p^2 \frac{V''}{V}, \quad (\text{A.5})$$

which are stable attractors under the condition

$$\epsilon \equiv \frac{M_p^2}{2} \left( \frac{V'}{V} \right)^2 \ll 1, \quad (\text{A.6})$$

and for a nearly constant  $\eta$  satisfying  $\eta \leq 3/4$ . Here, note that  $\eta$  is not bounded from below, and that  $\tilde{c} \geq 3/2$ . The familiar slow-roll approximations are recovered when  $|\eta| \ll 1$ . To be precise, inflation can happen even for  $\epsilon > 1$  given a large  $\tilde{c}$  (i.e. largely negative  $\eta$ ).<sup>18</sup> However in this appendix we limit our studies to curvaton potentials satisfying (A.6) at  $\sigma = \sigma_{\text{dom}}$ , as the hilltop potentials which are discussed in the next section satisfy this condition. Then, since the curvaton field value is monotonically increasing or decreasing in terms of time, we can use  $\sigma$  as a clock,

$$\mathcal{N}_b = \int_{\sigma_{\text{dom}}}^{\sigma_f} \frac{H}{\dot{\sigma}} d\sigma. \quad (\text{A.7})$$

Here, note that  $H/\dot{\sigma}$  is a function of  $\sigma$ , and since  $\rho_f$  is a constant among different patches of the universe, so is  $\sigma_f$ .<sup>19</sup> Hence by partially differentiating both sides in terms of  $\sigma_*$ , one obtains

$$\frac{\partial \mathcal{N}_b}{\partial \sigma_*} \simeq \frac{\tilde{c} V}{3M_p^2 V'} \Big|_{\sigma=\sigma_{\text{dom}}} \frac{\partial \sigma_{\text{dom}}}{\partial \sigma_*}. \quad (\text{A.8})$$

In order to compute  $\partial \sigma_{\text{dom}} / \partial \sigma_*$ , we make use of the slow-roll approximation  $3H\dot{\sigma} \simeq -V'$  while  $t \leq t_{\text{end}}$ . During  $t_{\text{end}} \leq t \leq t_{\text{dom}}$ , for simplification we treat the universe as a matter dominated

<sup>17</sup>This approximation is valid as long as the main contribution to  $\delta \mathcal{N}$  comes from the difference in the duration of the second inflation.

<sup>18</sup>The study on the stability of the rapid-roll attractor given in the appendix of [48] mainly considers  $\tilde{c} = \mathcal{O}(1)$ , but one can easily extend their discussions to cases with  $\tilde{c} \gg 1$ .

<sup>19</sup>Considering  $\rho_f \simeq V(\sigma_f)$ , then for a potential that monotonically increases or decreases in terms of  $\sigma$  during inflation, one sees that  $\sigma_f$  is a constant.

one and adopt  $\frac{9}{2}H\dot{\sigma} \simeq -V'$  (cf. (2.1), see also Footnote 17). Also using  $\dot{H}/H^2 = -3/2$  for  $t_{\text{end}} \leq t \leq t_{\text{dom}}$ , then one can check that

$$\int_{\sigma_*}^{\sigma_{\text{dom}}} \frac{d\sigma}{V'(\sigma)} \simeq \frac{4}{27} \int_{H_{\text{end}}}^{H_{\text{dom}}} \frac{dH}{H^3} + (\text{terms independent of } \sigma_*). \quad (\text{A.9})$$

Partially differentiating both sides by  $\sigma_*$ , and using  $3M_p^2 H_{\text{dom}}^2 \simeq 2V(\sigma_{\text{dom}})$ ,<sup>20</sup> one obtains

$$\frac{\partial \sigma_{\text{dom}}}{\partial \sigma_*} \simeq \frac{V'(\sigma_{\text{dom}})}{V'(\sigma_*)}, \quad (\text{A.10})$$

where we have dropped the contribution from the right hand side of (A.9) from the condition (A.6) satisfied at  $\sigma = \sigma_{\text{dom}}$ .

Combining the above results, we can calculate the density perturbation spectrum:

$$\mathcal{P}_\zeta = \left( \frac{\partial \mathcal{N}}{\partial \sigma_*} \right) \left( \frac{H_*}{2\pi} \right)^2, \quad (\text{A.11})$$

where (again using (A.6))

$$\frac{\partial \mathcal{N}}{\partial \sigma_*} \simeq \frac{\tilde{c}(\sigma_{\text{dom}})V(\sigma_{\text{dom}})}{3M_p^2 V'(\sigma_*)}. \quad (\text{A.12})$$

The spectral index follows as

$$n_s - 1 \simeq 2 \frac{\dot{H}_*}{H_*^2} + \frac{2}{3} \frac{V''(\sigma_*)}{H_*^2}, \quad (\text{A.13})$$

taking the same form as for non-inflating curvatons (2.9). The non-Gaussianity parameter can also be calculated:

$$f_{\text{NL}} = \frac{5}{6} \frac{\partial^2 \mathcal{N}}{\partial \sigma_*^2} \left( \frac{\partial \mathcal{N}}{\partial \sigma_*} \right)^{-2} \simeq \frac{5}{2\tilde{c}(\sigma_{\text{dom}})} \left\{ \left( \frac{M_p V'(\sigma_{\text{dom}})}{V(\sigma_{\text{dom}})} \right)^2 - \frac{M_p^2 V''(\sigma_*)}{V(\sigma_{\text{dom}})} \right\} + \dots, \quad (\text{A.14})$$

where  $\dots$  denotes terms proportional to  $\partial \tilde{c}(\sigma_{\text{dom}})/\partial \sigma_{\text{dom}}$ . One immediately sees that the first term in the  $\{ \}$  parentheses is much smaller than unity from the condition (A.6), while the second term can be larger than unity for rapid-roll inflation, i.e.  $|\eta| \gtrsim 1$ .

In the above discussion, we have considered the inflaton to decay after the curvaton domination. Similar computations can be carried out also for the case where the inflaton decays between the first and second inflationary periods, by approximating the universe as matter dominated while  $t_{\text{end}} \leq t \leq t_{\text{reh}}$  (here the subscript ‘‘reh’’ denotes values at  $H = \Gamma_\phi$ , when the inflaton is assumed to suddenly decay), and then radiation dominated while  $t_{\text{reh}} \leq t \leq t_{\text{dom}}$ . Further assuming the condition (A.6), and also that the tilt of the curvaton potential at  $\sigma_{\text{reh}}$  to be not much greater than at  $\sigma_{\text{dom}}$ , i.e.,

$$|V'(\sigma_{\text{reh}})| \lesssim |V'(\sigma_{\text{dom}})|, \quad (\text{A.15})$$

<sup>20</sup>This may seem contradicting with the slow/rapid-roll approximation (A.5)  $3M_p^2 H^2 \simeq V$ , but the numerical coefficient of  $V$  only affects a  $M_p^2 (V'/V)^2$  term which is dropped in the final expression (A.10), thus we will not worry about it.

then one obtains the same results (A.12), (A.13), and (A.14). Whether the inflaton decays before or after the curvaton domination has little effect since the density perturbations are sourced mainly through different patches of the universe experiencing slightly longer/shorter periods of the second inflation.

In summary, independently of whether the inflaton decays before/after the curvaton domination, under the condition (A.6) (and also (A.15) for  $t_{\text{reh}} < t_{\text{dom}}$ ), the linear perturbation sourced by inflating curvatons is of the form (A.11) with (A.12), the spectral index is (A.13), and the non-linearity parameter is given by (A.14).

## A.2 Inflating at the Hilltop

As an example, let us consider inflating curvatons with a hilltop potential

$$V(\sigma) = V_0 - \frac{1}{2}m^2(\sigma - \sigma_0)^2, \quad (\text{A.16})$$

where  $V_0$ ,  $m$ , and  $\sigma_0$  are constants. Given that the curvaton is located sufficiently close to the hilltop  $\sigma_0$  such that  $V_0 \gg m^2(\sigma - \sigma_0)^2$  and  $V_0^2 \gg M_p^2 m^4(\sigma - \sigma_0)^2$  until the curvaton starts driving inflation, then one finds

$$\frac{\partial \mathcal{N}}{\partial \sigma_*} \simeq -\frac{3 + \sqrt{9 - 12\eta}}{6\eta} \frac{1}{(\sigma_0 - \sigma_*)}, \quad (\text{A.17})$$

and

$$f_{\text{NL}} \simeq -\frac{5\eta}{2\bar{c}} = \frac{5}{12} \left( -3 + \sqrt{9 - 12\eta} \right), \quad (\text{A.18})$$

where

$$\eta \simeq -\frac{M_p^2 m^2}{V_0}. \quad (\text{A.19})$$

Note especially that  $\eta$  is (almost) a constant which is negative in this example. We also remark that we have dropped the contribution on  $f_{\text{NL}}$  from the first term in the parentheses of (A.14) which is clearly smaller than unity.

## A.3 Axionic Curvatons

In this final subsection, we look into axionic curvatons inflating at the hilltop of the potential (3.1). (We do not consider axionic curvatons away from the hilltop driving large-field inflation with super-Planckian decay constants  $f$ .) The discussions in Section A.2 can be applied to this case by simply substituting

$$V_0 = 2\Lambda^4, \quad m^2 = \frac{\Lambda^4}{f^2}, \quad \sigma_0 = f\pi. \quad (\text{A.20})$$

Then one can see that the negative  $\eta$  parameter is determined merely by the symmetry breaking scale  $f$  as

$$\eta \simeq -\frac{M_p^2}{2f^2}. \quad (\text{A.21})$$

Non-Gaussianities from inflating axionic curvatons are in general smaller compared to non-inflating cases, which can be seen from (A.18): Large  $f_{\text{NL}}$  requires a large, negative  $\eta$ , however

a large  $|\eta|$  substantially accelerates the curvaton thus makes it challenging for the curvaton to drive inflation in the first place. We show this explicitly in Figure 3, which investigates the parameter space of axionic curvatons beyond the allowed window for non-inflating axionic curvatons discussed in Section 3. Here we fix the curvaton mass to  $m_\sigma = \Lambda^2/f = 10^8$  GeV, and investigate large  $f$  values beyond the right blue edge (corresponding to the requirement that the curvaton be subdominant until it starts oscillating) in Figure 1. Using (A.13), we fix the (first) inflation scale  $H_{\text{inf}}$  from the spectral index  $n_s \approx 0.96$  assuming constant  $H$  during inflation, and also fix the curvaton position at CMB scale horizon exit  $\sigma_*/f$  from  $\mathcal{P}_\zeta \approx 2.4 \times 10^{-9}$  using (A.17). Furthermore, we set the number of e-foldings between the CMB scale horizon exit and the end of the (first) inflation as  $\mathcal{N}_* = 50$ , the curvaton decay rate  $\Gamma_\sigma$  by (3.3) with  $\beta = 1$ , and the inflaton decay rate  $\Gamma_\phi$  small enough such that the inflaton decays after the curvaton domination. (The explicit value of  $\Gamma_\phi$  is irrelevant for the density perturbations, however whether the inflaton decays before/after the curvaton domination slightly affects the number of e-folds obtained in the second inflation.) The resulting non-Gaussianity  $f_{\text{NL}}$  is plotted as a function of  $f$  in Figure 3, where the blue solid line denotes the analytic calculation (A.18) with (A.21). We have also numerically computed  $f_{\text{NL}}$ , whose results are shown as blue dots in the figures. One sees that the analytic and numerical results match well. In the right figure, we also show the number of e-folds  $\mathcal{N}_{\text{sec}}$  obtained in the second inflationary period driven by the axionic curvaton.  $\mathcal{N}_{\text{sec}}$  here is defined as the e-folding number from the curvaton domination until when the curvaton starts oscillating, i.e. (2.2). When the second inflationary period is very short, the analytic estimations derived in this appendix are invalid, which sources the slight difference between the analytic and numerical computations of  $f_{\text{NL}}$  at  $f \approx 10^{17.4}$  GeV. When further increasing  $f$  beyond the plotted regime,  $f_{\text{NL}}$  becomes further suppressed while  $\mathcal{N}_{\text{sec}}$  rapidly increases, soon making the axionic curvaton responsible for driving most of the inflationary e-folds after the CMB scale horizon exit. In summary, non-Gaussianity in the region beyond the right blue edge in Figure 3 decreases for larger  $f$ , taking values smaller than  $\sim 10$  in most of the region. Larger non-Gaussianity is generated when closer to the edge, i.e. when the second inflationary period is very short and the situation is close to the familiar non-inflating curvatons.

Let us also note that the power spectrum (A.17) is now written as

$$\mathcal{P}_\zeta^{1/2} \simeq \kappa \left(1 - \frac{\sigma_*}{\pi f}\right)^{-1} \frac{H_*}{M_p}, \quad \text{where} \quad \kappa \equiv \frac{3 + \sqrt{9 - 12\eta}}{6\pi^2 \sqrt{-2\eta}}. \quad (\text{A.22})$$

For a sub-Planckian  $f$  (i.e.  $f \leq M_p$ ), the prefactor  $\kappa$  can only take values within  $0.04 \lesssim \kappa \lesssim 0.12$ . Therefore, once the initial position of the curvaton  $\sigma_*/\pi f$  is given, the inflationary scale  $H_*$  needs to be tuned to a rather narrow scale range in order for an inflating axionic curvaton to source the linear perturbation with an appropriate amplitude. This is in contrast to non-inflating axionic curvatons, which can work with a wide range of inflationary scales for each value of  $\sigma_*/\pi f$  [10].

We remark that the inflating curvaton was studied in Ref. [49], however their results differ from ours. In particular, they claimed that the non-Gaussianity parameter  $f_{\text{NL}}$  is *negative* and of order unity<sup>21</sup>, while we have shown that  $f_{\text{NL}}$  from a hilltop curvaton is *positive* and can take values larger as well as smaller than order unity. Moreover we have confirmed our results for the case of axionic

<sup>21</sup>They assumed the curvaton mass to be much lighter than the Hubble parameter during inflation, but even in this case the analysis shown in Figure 3 does not change much since  $f_{\text{NL}}$  from an axionic curvaton is set merely by the decay constant  $f$ .

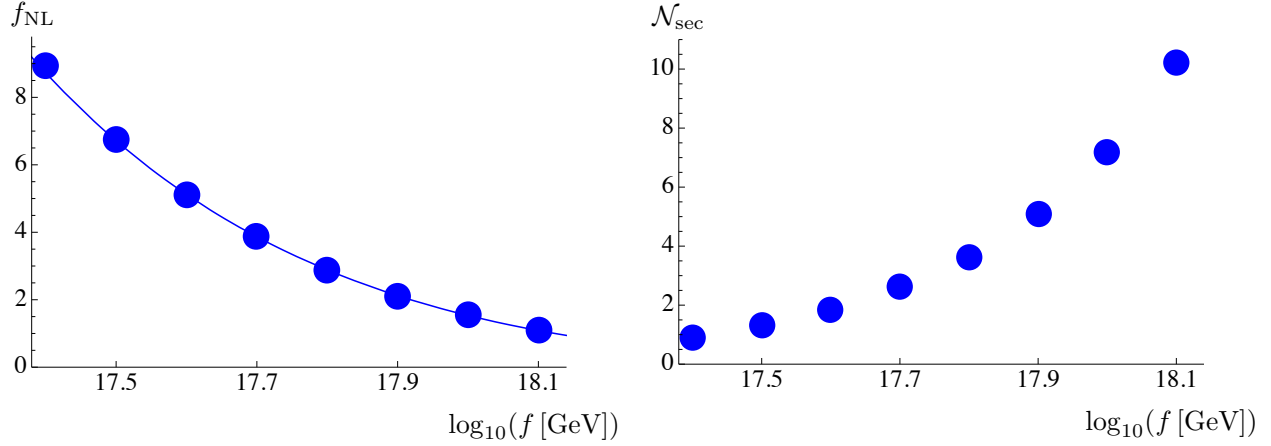


Figure 3: Left: Non-Gaussianity from an inflating axionic curvaton with a fixed mass  $m_\sigma = 10^8$  GeV, when increasing the decay constant  $f$  beyond the right blue edge of the allowed parameter window in Figure 1. Parameters other than  $m_\sigma$  and  $f$  are fixed from requiring  $\mathcal{P}_\zeta \approx 2.4 \times 10^{-9}$  and  $n_s \approx 0.96$ . Right: Number of e-folds in the second inflationary period driven by the axionic curvaton.

curvatons by numerical calculations as shown in Fig. 3, where one sees that  $f_{\text{NL}}$  varies from 9 to 1 as the e-folding number in the second inflation increases from 1 to 10.

## References

- [1] A. H. Guth, Phys. Rev. **D23**, 347-356 (1981); A. A. Starobinsky, Phys. Lett. B **91** (1980) 99; K. Sato, Mon. Not. Roy. Astron. Soc. **195**, 467-479 (1981).
- [2] E. Komatsu *et al.* [WMAP Collaboration], Astrophys. J. Suppl. **192** (2011) 18 [arXiv:1001.4538 [astro-ph.CO]].
- [3] A. D. Linde and V. F. Mukhanov, Phys. Rev. D **56**, 535 (1997) [arXiv:astro-ph/9610219].
- [4] K. Enqvist and M. S. Sloth, Nucl. Phys. B **626**, 395 (2002) [arXiv:hep-ph/0109214].
- [5] D. H. Lyth and D. Wands, Phys. Lett. B **524**, 5 (2002) [arXiv:hep-ph/0110002].
- [6] T. Moroi and T. Takahashi, Phys. Lett. B **522**, 215 (2001) [Erratum-ibid. B **539**, 303 (2002)] [arXiv:hep-ph/0110096].
- [7] G. Dvali, A. Gruzinov and M. Zaldarriaga, Phys. Rev. D **69**, 023505 (2004) [astro-ph/0303591].
- [8] L. Kofman, astro-ph/0303614.
- [9] A. Arvanitaki, S. Dimopoulos, S. Dubovsky, N. Kaloper and J. March-Russell, Phys. Rev. D **81**, 123530 (2010) [arXiv:0905.4720 [hep-th]].
- [10] M. Kawasaki, T. Kobayashi and F. Takahashi, Phys. Rev. D **84** (2011) 123506 [arXiv:1107.6011 [astro-ph.CO]].
- [11] M. Kawasaki, K. Nakayama and F. Takahashi, JCAP **0901**, 026 (2009) [arXiv:0810.1585 [hep-ph]].
- [12] G. Aad *et al.* [ATLAS Collaboration], Phys. Lett. B **716**, 1 (2012) [arXiv:1207.7214 [hep-ex]].
- [13] S. Chatrchyan *et al.* [CMS Collaboration], Phys. Lett. B **716**, 30 (2012) [arXiv:1207.7235 [hep-ex]].
- [14] I. L. Bogolyubsky and V. G. Makhankov, Pisma Zh. Eksp. Teor. Fiz. **24**, 15 (1976).
- [15] I. L. Bogolyubsky and V. G. Makhankov, JETP Lett. **24**, 12 (1976).
- [16] M. Gleiser, Phys. Rev. D **49**, 2978 (1994) [hep-ph/9308279].
- [17] E. J. Copeland, M. Gleiser and H. -R. Muller, Phys. Rev. D **52**, 1920 (1995) [hep-ph/9503217].
- [18] S. Kasuya, M. Kawasaki and F. Takahashi, Phys. Lett. B **559**, 99 (2003) [hep-ph/0209358].
- [19] A. A. Starobinsky, JETP Lett. **42**, 152 (1985) [Pisma Zh. Eksp. Teor. Fiz. **42**, 124 (1985)].
- [20] M. Sasaki and E. D. Stewart, Prog. Theor. Phys. **95**, 71 (1996) [astro-ph/9507001].
- [21] D. Wands, K. A. Malik, D. H. Lyth and A. R. Liddle, Phys. Rev. D **62**, 043527 (2000) [astro-ph/0003278].

- [22] D. H. Lyth, K. A. Malik and M. Sasaki, JCAP **0505**, 004 (2005) [astro-ph/0411220].
- [23] E. Komatsu and D. N. Spergel, Phys. Rev. D **63**, 063002 (2001) [astro-ph/0005036].
- [24] C. T. Byrnes, K. Enqvist and T. Takahashi, JCAP **1009**, 026 (2010) [arXiv:1007.5148 [astro-ph.CO]].
- [25] C. T. Byrnes, K. Enqvist, S. Nurmi and T. Takahashi, JCAP **1111**, 011 (2011) [arXiv:1108.2708 [astro-ph.CO]].
- [26] T. Kobayashi and T. Takahashi, JCAP **1206**, 004 (2012) [arXiv:1203.3011 [astro-ph.CO]].
- [27] D. H. Lyth, Phys. Rev. Lett. **78**, 1861 (1997) [hep-ph/9606387].
- [28] I. Ben-Dayan and R. Brustein, JCAP **1009**, 007 (2010) [arXiv:0907.2384 [astro-ph.CO]].
- [29] K. Dimopoulos, D. H. Lyth, A. Notari and A. Riotto, JHEP **0307**, 053 (2003) [hep-ph/0304050].
- [30] M. Kawasaki, K. Kohri, N. Sugiyama, Phys. Rev. Lett. **82**, 4168 (1999). [astro-ph/9811437].
- [31] M. Kawasaki, K. Kohri, N. Sugiyama, Phys. Rev. **D62**, 023506 (2000). [astro-ph/0002127].
- [32] S. Hannestad, Phys. Rev. D **70**, 043506 (2004).
- [33] K. Ichikawa, M. Kawasaki and F. Takahashi, Phys. Rev. D **72**, 043522 (2005).
- [34] E. W. Kolb, A. Notari and A. Riotto, Phys. Rev. D **68**, 123505 (2003) [arXiv:hep-ph/0307241].
- [35] J. Yokoyama, Phys. Lett. B **635**, 66 (2006) [arXiv:hep-ph/0510091].
- [36] M. Drewes, arXiv:1012.5380 [hep-th].
- [37] Y. Okada, M. Yamaguchi and T. Yanagida, Phys. Lett. B **262**, 54 (1991);  
see also Y. Okada, M. Yamaguchi and T. Yanagida, Prog. Theor. Phys. **85**, 1 (1991);  
J. R. Ellis, G. Ridolfi and F. Zwirner, Phys. Lett. B **257**, 83 (1991);  
H. E. Haber and R. Hempfling, Phys. Rev. Lett. **66**, 1815 (1991).
- [38] G. F. Giudice and A. Strumia, Nucl. Phys. B **858**, 63 (2012) [arXiv:1108.6077 [hep-ph]];  
G. Degrandi, S. Di Vita, J. Elias-Miro, J. R. Espinosa, G. F. Giudice, G. Isidori and A. Strumia,  
JHEP **1208**, 098 (2012) [arXiv:1205.6497 [hep-ph]];  
see also F. Bezrukov, M. Y. Kalmykov, B. A. Kniehl and M. Shaposhnikov, arXiv:1205.2893  
[hep-ph].
- [39] S. Kachru, R. Kallosh, A. D. Linde and S. P. Trivedi, Phys. Rev. D **68**, 046005 (2003) [hep-th/0301240].
- [40] K. Nakayama and F. Takahashi, arXiv:1206.3191 [hep-ph].
- [41] K. Hamaguchi, M. Kawasaki, T. Moroi and F. Takahashi, Phys. Rev. D **69**, 063504 (2004) [hep-ph/0308174].



- [42] I. Affleck and M. Dine, Nucl. Phys. B **249**, 361 (1985).
- [43] M. Dine, L. Randall, S. D. Thomas, Phys. Rev. Lett. **75** 398 (1995) [arXiv:hep-ph/9503303];  
M. Dine, L. Randall and S. D. Thomas, Nucl. Phys. B **458**, 291 (1996) [arXiv:hep-ph/9507453].
- [44] A. D. Linde, JHEP **0111**, 052 (2001) [hep-th/0110195].
- [45] L. Boubekour and D. H. Lyth, JCAP **0507**, 010 (2005) [hep-ph/0502047].
- [46] W. H. Kinney, Phys. Rev. D **72**, 023515 (2005) [gr-qc/0503017].
- [47] K. Tzirakis and W. H. Kinney, Phys. Rev. D **75**, 123510 (2007) [astro-ph/0701432].
- [48] T. Kobayashi, S. Mukohyama and B. A. Powell, JCAP **0909**, 023 (2009) [arXiv:0905.1752 [astro-ph.CO]].
- [49] K. Dimopoulos, K. Kohri, D. H. Lyth and T. Matsuda, JCAP **1203**, 022 (2012) [arXiv:1110.2951 [astro-ph.CO]].